Molecular Crystals and Liquid Crystals Science and Technology. Section A. Molecular Crystals and Liquid Crystals

Publication details, including instructions for authors and subscription information:
http://www.tandfonline.com/loi/gmcl19

Third-Order Nonlinearities in Organic Polymers and the Role of Microscopic Cascading of Second-Order Hyperpolarizabilities

Gaetano Assanto [a], Dieter Neher [a], George I. Stegeman [a], William E. Torruellas [b], Manuel B. Marques [c], Winfried H. G. Horsthuis [d] & Guus R. Möhlmann [d]

[a] CREOL, University of Central Florida, Orlando, FL, 32826, USA

[b] Raytheon Research Division, 131 Spring Street, Lexington, MS, 02173, USA

[c] Centro de Fisica da Universidade do Porto (INIC), 4000, Porto, Portugal

[d] AKZO Research Laboratories, Arnhem, P.O. Box 9300, 6800, SB Arnhem, The Netherlands

Version of record first published: 04 Oct 2006.

To cite this article: Gaetano Assanto , Dieter Neher , George I. Stegeman , William E. Torruellas , Manuel B. Marques , Winfried H. G. Horsthuis & Guus R. Möhlmann (1992): Third-Order Nonlinearities in Organic Polymers and the Role of Microscopic Cascading of Second-Order Hyperpolarizabilities, Molecular Crystals and Liquid Crystals Science and Technology. Section A. Molecular Crystals and Liquid Crystals, 222:1, 33-43

To link to this article: http://dx.doi.org/10.1080/15421409208048678

Mol. Cryst. Liq. Cryst. 1992, Vol. 222, pp. 33–43
Reprints available directly from the publisher
Photocopying permitted by license only

Printed in the United States of America

THIRD-ORDER NONLINEARITIES IN ORGANIC POLYMERS AND THE ROLE OF MICROSCOPIC CASCADING OF SECOND-ORDER HYPERPOLARIZABILITIES

Gaetano ASSANTO, Dieter NEHER and George I. STEGEMAN
CREOL, University of Central Florida, Orlando, FL 32826 (USA)

William E. TORRUELLAS
Raytheon Research Division, 131 Spring Street, Lexington, MS 02173 (USA)

Manuel B. MARQUES
Centro de Fisica da Universidade do Porto (INIC), 4000 Porto, Portugal

Winfried H.G. HORSTHUIS and Guus R. MÖHLMANN
AKZO Research Laboratories, Arnhem, P.O. Box 9300, 6800 SB Arnhem, The Netherlands

(Received October 4, 1991)

Abstract We investigate the third-order nonlinearity of DANS and DAN2 side-chain polymers by tunable third-harmonic generation and nonlinear distributed coupling. The large third-order susceptibility can be interpreted in terms of microscopic cascading of second-order hyperpolarizabilities.

INTRODUCTION

The successful implementation of devices for all-optical signal processing and optical computing in integrated optics formats requires highly nonlinear materials with properties suitable for waveguide fabrication. Polymers can exhibit both large and fast nonresonant third-order nonlinearities which rely on π-electron delocalization and conjugation, as well as good physical and chemical properties suitable for the fabrication of nonlinear integrated optics devices.[1]

Soluble polymers with strong charge transfer states such asymmetrically substituted 4-dialkylamino-4′-nitro-stilbene (DANS) and 4-dialkylamino-4′-nitro-diphenylbutadiene (DAN2) side-groups (see Fig.1) were originally developed for electro-optic applications because of their large second order nonlinearities and low propagation losses in waveguide format.[2] They represent a new approach to achieving third order nonlinearities based on charge transfer states and local cascading of second order nonlinearities.[3]

Cascading at a frequency ω occurs when a local field at the second harmonic due to $\beta^{(2)}(-2\omega,\omega,\omega)E(\omega)^2$ mixes with the fundamental field via $\beta^{(2)}(-\omega,2\omega,-\omega)E(2\omega)E^*(\omega)$ to produce a field at ω. This leads to an index change proportional to

$\beta^{(2)}(-\omega;2\omega,-\omega)\beta^{(2)}(-2\omega;\omega,\omega)|E(\omega)|^2 E(\omega)$. The contribution to n_2 scales quadratically with the magnitude of the second order hyperpolarizability, hence the name "cascading nonlinearity". When $\beta^{(2)}(-3\omega;2\omega,\omega)$ is involved, cascading contributes to the enhancement of the generated third-harmonic. Note that since the mechanism is operative at a molecular level,[3] this nonlinearity still occurs with randomly oriented molecules for which there is no net macroscopic second order susceptibility.

DANS

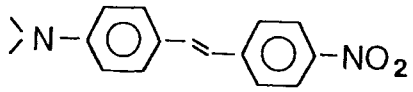

DAN2

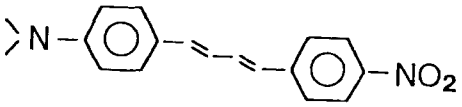

FIGURE 1 Molecular structure of DANS and DAN2 active moieties.

In order to evaluate the third-order nonlinear susceptibility of these polymers in a thin film form, we have employed two techniques: nonlinear grating coupling, which allows to estimate size and sign of the Kerr coefficient n_2,[4] and tunable third-harmonic generation (THG), which enables to measure the dispersion of $\chi^{(3)}(-3\omega;\omega,\omega,\omega)$.[5] Our measurements and analyses show large electronic non-resonant $\chi^{(3)}$ values, comparable to some of the best values obtained to date for soluble conjugated polymers. We show that, depending upon the theoretical model adopted, the results might indicate a significant contribution of the local cascading of second order hyperpolarizabilities to the third-order nonlinearity.[3]

PREPARATION OF THIN FILM SAMPLES

Planar waveguides were realized by spin-coating the materials from a filtered (0.2μm pore size) cyclopentanone solution (typically 23% by mass) onto fused-silica substrates, ultrasonically pre-cleaned and with two coupling gratings on the glass surface. After spinning, the samples were cured on a hot plate in air at 140°C for about 60 minutes. The gratings, fabricated by ion-milling in Freon through holographic photoresist masks, had a periodicity Λ=0.6 μm.

The linear properties of the films were characterized by evaluating thickness and refractive indices via linear coupling into various guided modes and then inverting the dispersion

relation for a three-layer planar structure. Indices at 1.064μm were $\simeq$1.62 for DANS and 1.64 for DAN2. The propagation losses were quantified by measuring the out-of-plane scattering along the propagation path, using a coherent fiber-bundle and a detector with data-acquisition hardware and software. The absorption in the visible was measured by standard white-light spectrophotometry, and the spectra are reproduced in Fig. 2. The red-shift attributable to the elongation of the conjugated system is visible in the graphs. The propagation losses (absorption + scattering) in these particular samples are relatively high due to scattering at the interfaces, between 6 and 18 dB/cm. Much lower losses (<1 dB/cm at 1.3 μm) have been obtained with these materials fabricated into channel waveguides in sandwich structures with polymer buffer layers.[2]

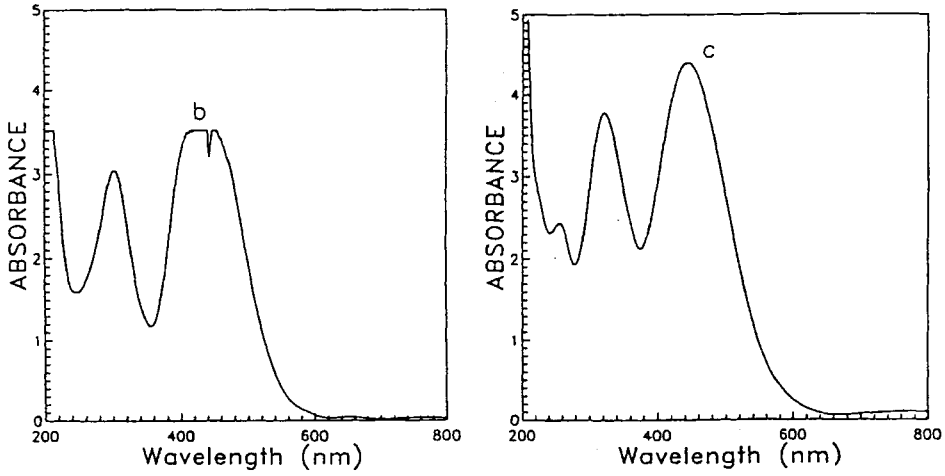

FIGURE 2 Absorption spectra of a) DANS and b) DAN2. The absorbance is normalized to 1μm. The peak absorbance in a) saturated the spectrophotometer response due to the larger thickness.

TUNABLE THIRD HARMONIC GENERATION MEASUREMENTS

We used a 10Hz Q-switched Nd-Yag laser at 1.064μm, doubled to 532nm, to pump an amplified dye laser with either Rhodamine 6G or DCM dyes. The IR beam and the visible radiation were then mixed in $LiIO_3$ to obtain tunable infrared in the 1.45-1.75μm range. Longer wavelengths, up to 1.904μm, were generated using a 1m-long H_2-filled Raman cell at 20atm.

For the measurements, we adopted a standard Maker fringe geometry, focussing pulses of 25 to 250μJ into a vacuum chamber containing the sample, with the thin film layer facing the detector (photomultiplier) and light vertically polarized with respect to the plane of incidence. The vacuum cell allowed us to reduce the error in the data, and to prevent oxygen-assisted photodegradation to take place during the measurements. Precise values for magnitude and phase of $\chi^{(3)}(3\omega;\omega,\omega,\omega)$ were derived from the Maker fringe data by comparing the THG results with those collected after complete removal of the organic compounds from the fused silica substrate, and repeating the experiment at exactly the same location on the sample.[5,8] A typical example of the collected data is shown in Fig.3. We also show some fits obtained by the simplex method using the formula by Kajzar,[7] not including the effect of multiple reflections of the THG light in the structure.

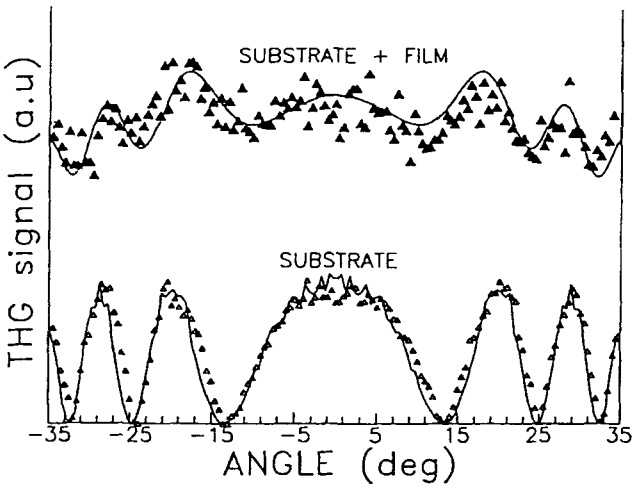

FIGURE 3 THG Maker fringes and corresponding theoretical fits at 1.904μm, for the substrate and the film+substrate cases, using DAN2. The lower data and line are magnified to allow for a visual comparison.

Figure 4 presents the experimentally determined magnitude of $\chi^{(3)}(3\omega)$ for a DANS side-chain polymer relative to the third-order susceptibility of fused-silica. The error bars are due to multiple reflections effects. The values, converted to n_2 units, are $|n_2|=4.3\cdot10^{-8}$ and $7.7\cdot10^{-8}$ cm^2/MW at 1.904 and 1.579 μm, respectively, for DANS, and $|n_2|=7\cdot10^{-8}$ and $1.05\cdot10^{-7}$ cm^2/MW at the same wavelengths for DAN2.Figure 5 shows the corresponding relative phase of $\chi^{(3)}$ versus wavelength for DANS.

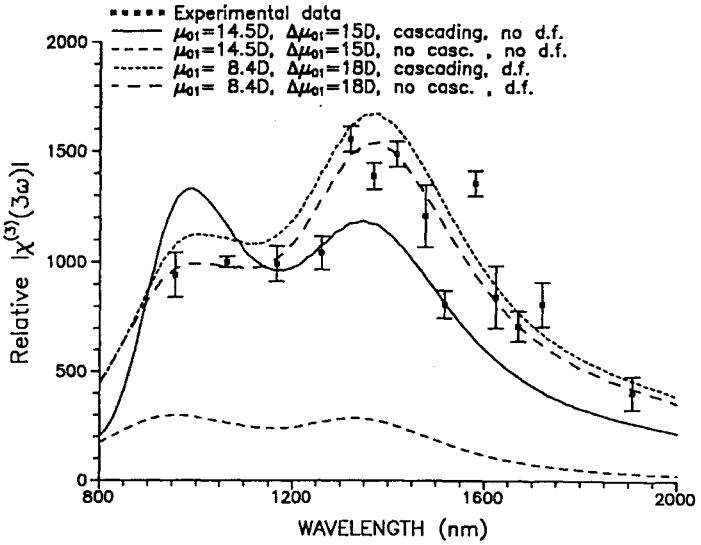

FIGURE 4 Measurement of the spectral dispersion of the relative size of $\chi^{(3)}(-3\omega;\omega,\omega,\omega)$ for a DANS sample (squares with error bars). The line fits were obtained with and without the cascading term, with and without a degeneracy factor (d.f.).

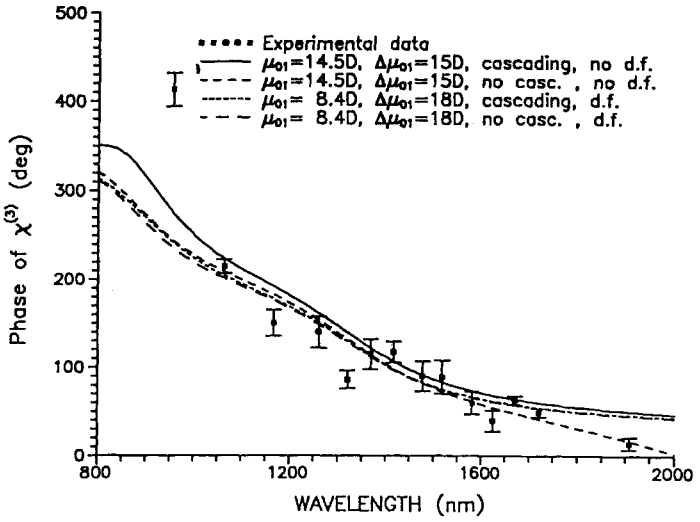

FIGURE 5 Spectral dispersion of the relative phase of $\chi^{(3)}(-3\omega;\omega,\omega,\omega)$ for the same DANS sample as in Fig.4. The various fitting curves tend to overlap.

NONLINEAR GRATING COUPLING EXPERIMENTS

This technique has been analysed in detail using a coupled-mode approach to relate the non-

linearity to the experimental observables.[4] In short, since an intensity driven change in index $\Delta n=n_2 \cdot I$ in the film affects the effective index of the waveguide mode and the corresponding wavevector, this change can be evaluated by input coupling via a surface relief grating. A typical experimental geometry is depicted in Figure 6. Because phase-matching between radiation and guided modes is the key to efficient excitation, a Kerr nonlinear wavevector detuning

$$k_0 \Delta n_{eff}(P_g) = k_0 n_{2eff} \cdot P_g \tag{1}$$

between the beam incident at an angle θ at a wavelength $\lambda=2\pi/k_0$, and the guided mode of power P_g can be quantified using the input grating coupler. n_{2eff} is an effective Kerr coefficient that takes into account the transverse guided field distribution in the slab.[4]

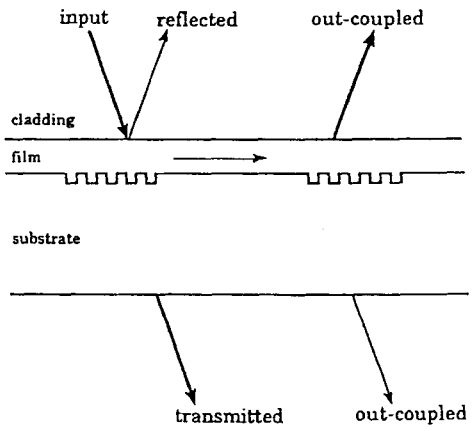

FIGURE 6 Schematic of the grating coupler geometry employed for the nonlinear measurement at $\lambda=1.064\mu m$.

When employing nonlinear grating coupling (NGC) for evaluating n_2, three principal results must be underlined:

1) When the incidence angle is set so that the low power in-coupling is optimized, the coupling efficiency decreases with increasing pulse power.

2) When the input angle is varied at fixed incident power, the angle at which the optimum coupling occurs varies with power.

3) Two photon absorption affects primarily throughput experiments.

To perform the nonlinear grating measurements, we used a Q-switched mode-locked Nd-YAG laser operating at 1.064 μm . The pulses, of duration Δt=30 ps at a repetition rate of 10 Hz, were measured before and after the sample using Si detectors and a Boxcar averager. The two output signals were the light coupled out from the second grating after propagation from the input to the output grating, and the light transmitted through the sample at the input grating.

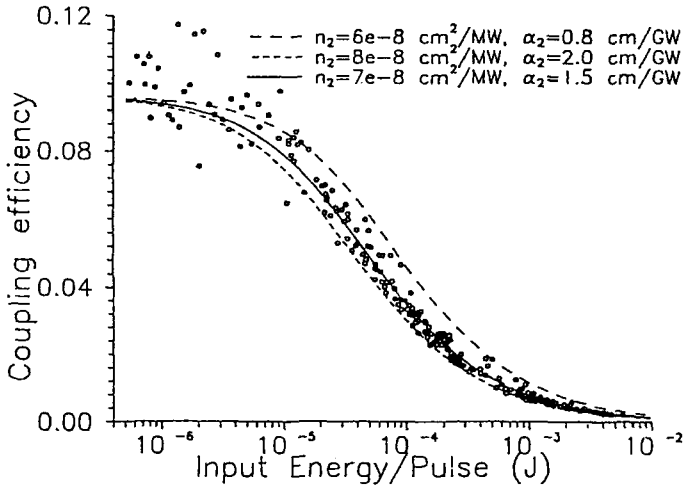

FIGURE 7 Throughput efficiency versus input pulse energies for a DANS sample. The circles are experimental data points, while the curves are calculations performed according to the numerical model. n_2=6·10^{-8} cm^2/MW, α_2=0.8 cm/GW for the long-dashed line, n_2=8·10^{-8} cm^2/MW and α_2=2.0 cm/GW short dashes, n_2=7·10^{-8} cm^2/MW and α_2=1.5 cm/GW the solid line.

Figure 7 shows some typical experimental data collected via the output grating of a DANS waveguide with the input coupler set at $\Delta\beta_0$=0 and an input beam diameter (FWHM) w_0=3.5 mm. The low power input coupling efficiencies η ranged between 10 and 17% in all the samples. The results in Fig.7 exhibit the characteristic limiting effect expected in a NGC as the input power is increased into a waveguide with reactive Kerr and TPA nonlinearities.

In Figure 8 we present the measured coupling efficiency versus coupling angle in DANS, for fixed excitation energies. Clearly, when the input power is increased, the coupling dip shifts towards smaller (negative) angles, with $\Delta\theta$>0. This indicates that n_2 is positive. The measured angular shifts were $\Delta\theta\simeq$+0.015^0 for DANS and $\simeq$+0.040^0 for DAN2, when the pulse energy was increased from 5 μJ to 350 or 500 μJ, respectively.

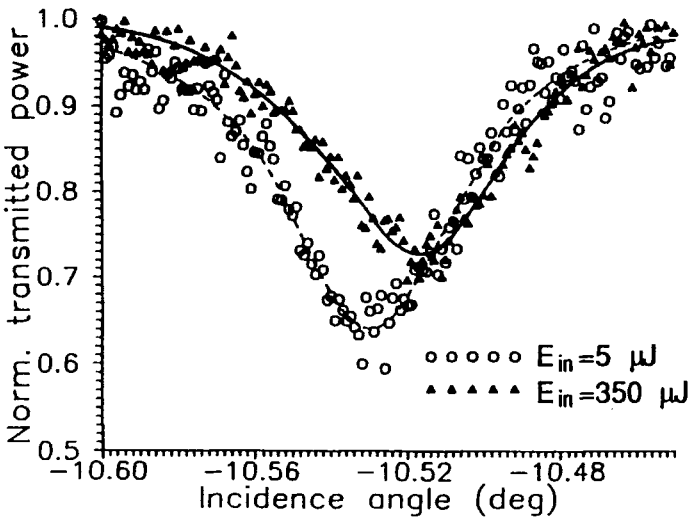

FIGURE 8 Normalized transmitted power through the input grating versus incidence angle for a DANS waveguide at low (5μJ, circles) and high (350μJ, triangles) input energies. The lines are meant to be a guide to the eye. The angular shift is ≃ +0.015°.

For the analysis, we followed the approach detailed in Ref.4, adjusting the low-power coupling efficiency η to the measured value and assuming temporal and spatial Gaussian shape for the beam. A purely Kerr nonlinearity (n_2) was initially assumed in analysing the angular shifts of the type shown in Fig. 8. With this value of n_2, we fitted the data collected via the output grating (Fig. 7), including the effects of TPA at both the input coupler and along the propagation path between the two gratings. Examples of theoretical curves are the lines also plotted in Fig.7. The procedure yielded n_2 and TPA values of $+7\pm1\times10^{-8}$ cm²/MW and 0.8-2 cm/GW for DANS, and $n_2\simeq+1.9\pm0.1\times10^{-7}$ cm²/MW and $\alpha_2\simeq$1-2 cm/GW for DAN2.[6]

To rule out the thermal effects, we estimated numerically the expected changes in η for a thermo-optic waveguide. Using typical polymer parameters and a material absorption (versus scattering) coefficient of 2 cm^{-1}, we calculated that a thermal nonlinearity would require input pulse energies significantly larger than those used in our NGC experiments. We conclude that the phenomena observed are primarily of electronic origin.

THE ROLE OF MICROSCOPIC CASCADING

The non-centrosymmetry of the molecules under consideration is an important characteristic of these systems, because it allows additional terms to contribute to the net third order sus-

ceptibility. Assuming that a two-level model with permanent dipole-moments in both the ground and excited state is appropriate, the resulting macroscopic susceptibility is:[3]

$$\chi^{(3)}(-3\omega;\omega,\omega,\omega) = N\,F\,\langle a_{iI}a_{jJ}a_{kK}a_{qQ}\rangle \cdot \tag{2}$$

$$[-\mu_{01}^4 D_{11}(\omega) + \mu_{01}^2\Delta\mu_{10}^2 D_{111}(\omega) + 2C\,\beta(-2\omega;\omega,\omega)\beta(-3\omega;2\omega,\omega)],$$

where N is the number density of molecules ($N=10^{21}$ cm^{-3}), μ_{01} is the transition dipole moment between the two-levels along the molecular axis, $\Delta\mu_{01}$ is the difference between the permanent dipole moments of the two states, F is the local field-factor function according to the Lorentz-Lorentz-model and the D's are the complex resonant denominators, calculated using the diagrammatic model[9]. C is the local field cascading factor defined by:

$$C = \frac{8\pi}{9v}\,\frac{[n^2(2\omega) - 1][n^2(2\omega) + 2]}{3n^2(2\omega)} \tag{3}$$

with v the volume of a sphere representing the molecule. The second and third terms in (2) are only allowed in molecules lacking a center of symmetry, while the last term induces a polarization at 3ω by mixing those at ω and 2ω. While all terms in (2) include similar resonant denominators, their relative contributions and thereby the role of cascading vary strongly with the values of μ_{01} and $\Delta\mu_{01}$.

To ascertain the role of cascading we fitted the experimental data in Fig.4 and Fig.5 using two different approaches. In the original fit to the data [5] the transition dipole moment μ_{01} was calculated to be 14.5D by integrating over the film absorption spectrum (neglecting local field effects). The volume v was set equal to 1/N. The fit with $\Delta\mu_{01}$ as the only adjustable parameter gave a value of $\Delta\mu_{01}$=15D comparable to the literature value[10]. The theoretical fits shown in Figs.4-5 show only fair agreement to the measured dispersion of $\chi^{(3)}$. A large cascading contribution similar to that generated by the intrinsic third-order susceptibility alone follows from the large value for the transition dipole moment relative to that for $\Delta\mu_{01}$.

In a second approach we used the established solvatochromic values μ_{01}=8.4D and $\Delta\mu_{01}$=18D.[10-11] According to a general approach the volume v was now approximated by a sphere with the cavity diameter equal to 0.7 times the length of the molecule[10-11]. With this set of parameters initially we were not able to explain the experimentally determined magnitude of $\chi^{(3)}(-3\omega;\omega,\omega,\omega)$. Agreement with the data was obtained by including frequency degeneracy factors of 2 and 6 for $\beta(-2\omega;\omega,\omega)$ and $\chi^{(3)}(-3\omega;\omega,\omega,\omega)$ respectively[9]. This

approach is justified by the fact that experimental values for $\beta(-2\omega;\omega,\omega)$ are often found to be a factor of 2 larger than those calculated from the solvatochromic data. These fits as shown in Figs.4-5 (long and short dashed lines) contain no adjustable parameters, and the contribution from cascading is almost negligible, mainly because of the much smaller transition dipole moment used in this approach. The calculated phase of $\chi^{(3)}$ is in both cases close to the measured values, confirming the validity of these two-level model approaches. We should emphasize that the use of frequency degeneracy factors is not common in the interpretation of experimental data. Nevertheless the good agreement with the experimental data makes the latter approach worth considering.

Conclusions

Nonlinear grating coupling measurements of the Kerr coefficient n_2 and tunable third-harmonic generation in a novel class of polymers with asymmetrically substituted side-chains have been performed on DANS and DAN2 thin films. These materials have shown large nonresonant third-order susceptibilities of electronic nature which make them good candidates for the realization of integrated all-optical devices. The analysis of the spectral dispersion of $\chi^{(3)}$, based on a two-level model, seems to point to the role of microscopic cascading of second-order hyperpolarizabilities in enhancing the third-order phenomena, both at the third harmonic and in degenerate four-wave interactions such as the optical Kerr effect. However, the interpretation of the data critically depends upon the theoretical model adopted. Further work is clearly required to establish a valid model for describing nonlinear susceptibilities in this class of materials.

This research was supported in USA by AFOSR (91-0339) and NSF (ECS-8911960).

References

1. G.I. Stegeman, C.T. Seaton, and R. Zanoni, Thin Solid Films 152, 231 (1987).
2. G.R. Möhlmann, W.H.G. Horstuis, C.P.J.M. van der Vorst, A.Mc. Donach, M. Copeland, C. Duchet, P. Fabre, M.B.J. Diemeer, E.S. Trommel, F.M.M. Suyten, P. Van Daele, E. Van Tomme, and R. Baets, SPIE Proc. V.1147, 245 (1989).
3. G.R. Meredith, Chem.Phys.Lett. 92, 165 (1982).
4. G. Assanto, M.B. Marques, and G.I. Stegeman, J.Opt.Soc.Am. B 8, 553 (1991).
5. W.E. Torruellas, R. Zanoni, G.I. Stegeman, G.R. Möhlmann, E.W.P. Erdhuisen, and W.H.G. Horstuis, J. Chem. Phys. 94, 6851 (1991).
6. M.B. Marques, G. Assanto, G.I. Stegeman, G.R. Möhlmann, E.W.P. Erdhuisen, and W.H.G. Horsthuis, Appl.Phys.Lett. 58, 2613 (1991).
7. F. Kajzar, J. Messier, and C. Rosilio, J.Appl.Phys. 60, 9 (1986).

8. W.E. Torruellas, R. Zanoni, M.B. Marques, G.I. Stegeman, G.R. Möhlmann, E.W.P. Erdhuisen, and W.H.G. Horstuis, Chem.Phys.Lett. 175, 267 (1990).
9. Y.R. Shen, "Principles of Nonlinear Optics", John Wiley and Sons Inc., New York (1984)
10. M.S. Paley, J.M. Harris, H. Looser, J.C. Baumert, G.C. Bjorklund, D. Jundt, R.J. Twieg, J.Org.Chem. 54, 3774 (1989).
11. W. Liptay, Angew. Chem. Internat. Edit. 8, 177 (1969).